

- (9) Erman, B.; Flory, P. J. *Macromolecules* 1983, 16, 1607.
 (10) Flory, P. J. *Proc. R. Soc. London, A* 1976, 351, 351.
 (11) Flory, P. J. *J. Chem. Phys.* 1977, 66, 5720.
 (12) Nagai, K. *J. Chem. Phys.* 1964, 40, 2818.
 (13) The orientation function is a second order tensor. It can be expressed in tensor form in terms of principal coordinates as

$$\mathbf{s} = D(\Delta\Lambda^2 + e\Delta\Theta^2)$$

where $\Delta\Lambda^2 = (3/2)(\Lambda^2 - \mathbf{I} \text{ tr } \Lambda^2/3)$ and $\Delta\Theta^2 = (3/2)(\Theta^2 - \mathbf{I} \text{ tr } \Theta^2/3)$, tr and \mathbf{I} denoting the trace operator and the identity

- matrix, respectively. The three diagonal components of \mathbf{s} in terms of principal coordinates are S_x , S_y , and S_z , the first of which is treated only in the present analysis.
 (14) Liberman, M. H.; Abe, Y.; Flory, P. J. *Macromolecules* 1972, 5, 550.
 (15) Flory, P. J. *Rubber Chem. Technol.* 1975, 48, 513.
 (16) Clement, C. B.; Bothorel, P. J. *Chim. Phys. Phys. Chim. Biol.* 1964, 61, 878.
 (17) Flory, P. J. *Faraday Discuss. R. Soc. Chem.* 1979, 68, 14.
 (18) Queslel, J.-P.; Erman, B.; Monnerie, L. *Macromolecules*, following paper in this issue.

Experimental Determination of Segmental Orientation in Polyisoprene Networks by Fluorescence Polarization and Comparison with Theory[†]

Jean-Pierre Queslel, Burak Erman,[‡] and Lucien Monnerie*

Laboratoire de Physicochimie Structurale et Macromoléculaire, Associé au CNRS, ESPCI, 75231 Paris Cedex 05, France. Received December 27, 1984

ABSTRACT: Segmental orientation is determined in deformed polyisoprene networks, in equilibrium, containing fluorescent anthracene labels attached to the middle of precursor chains and randomly located between cross-links. Measurements show that orientation depends nonaffinely on macroscopic strain, is not proportional to stress, and decreases rapidly with increasing temperature and dilution. Comparison of results with predictions of the theory based on the real network model shows that observed segmental orientation results from the joint contribution of nonaffine transformations of chains upon deformation and of distortion of the junction constraint domains. Strong temperature and swelling dependence of segmental orientation at all levels of deformation is attributed to local intermolecular correlations of segments.

Introduction

Orientation of segments in an amorphous network results from the deformations of chains under stress. In previous formulations of segmental orientation cited in the preceding paper¹ (referred to as I hereafter), chains have been assumed to deform affinely with the macroscopic strain. Recent experimental work on birefringence², and on fluorescence polarization^{3,4} of deformed networks has shown that deviations of segmental orientation from the predictions of the affine model are significant. Furthermore, these experiments have shown that local intermolecular orientational correlations of segments with their neighbors contribute to orientation.

Discrepancies between experimental measurements of strain birefringence and the existing affine theories have recently been reviewed.⁵ Analysis of the phenomenon of birefringence in terms of the real network model, in which chains transform nonaffinely with macroscopic strain, led to results that were in satisfactory agreement with those of experiment. In the preceding theoretical treatment¹ of segment orientation, similar corrections are applied to the commonly used freely jointed affinely deforming chain model. The resulting expression for the orientation function is seen to be the product of two terms, one showing the effect of individual chain properties, referred to as the configurational factor, the other describing the dependence on macroscopic strain, referred to as the strain function. Additional contributions to orientation, due to local intermolecular correlations, are incorporated into the configurational factor, as suggested by birefringence and

fluorescence polarization experiments.

With improved techniques of experimental spectroscopy,^{6,7} the magnitude of the configurational factor and the form of the strain function for amorphous networks may be determined accurately. In this study we report results of fluorescence spectroscopy on polyisoprene networks under uniaxial tension and compare them with predictions of the theory. The networks used contain a small number of chains labeled with a fluorescent group (anthracene), the orientation of which is determined by the measurement of fluorescence polarization induced upon deformation.

Materials and Methods

Samples were generously provided by Manufacture Michelin. Unimodal networks (samples A and B) were formed from an anionic commercial polyisoprene Shell IR 307 with a high cis-1,4 configuration (92% cis, 5% trans) ($T_g(\text{DSC}) = -60^\circ\text{C}$) of high molecular weight ($M_n = 46.3 \times 10^4$, $M_w = 182 \times 10^4$).

Bimodal networks (samples C and D) were formed from blends of 75% w/w IR 307 and 25% polyisoprene chains of low molecular weight ($M_n = 50\,000$), the microstructure of which is similar to that of IR 307.

Labeled anionic polyisoprene chains were prepared by using a method analogous to that reported previously for polystyrene.⁸ Monofunctional "living" chains of molecular weight 300 000 were synthesized and deactivated by 9,10-bis(bromomethyl)anthracene. Each of the resulting chains of double molecular weight contains a dimethylantracene (DMA) fluorescent group at its center. Thus the fluorescent transition moment, the orientation of which is measured, lies along the chain axis.

The labeled polymer (1%) and the matrix (99%), carefully purified by extraction with ethanol, were mixed in solution. Samples were molded and cross-linked with dicumyl peroxide. Curing time and temperature were adjusted to get different cross-linking densities, which were characterized by the average molecular weight M_c of network chains (between adjacent junctions) derived from measurements of the equilibrium swelling ratio in cyclohexane and through the classical Flory-Rehner equation.

[†] This paper is dedicated to Dr. Pierre Thirion on the occasion of his retirement.

[‡] Permanent address: Bogazici University, Bebek, Istanbul, Turkey.

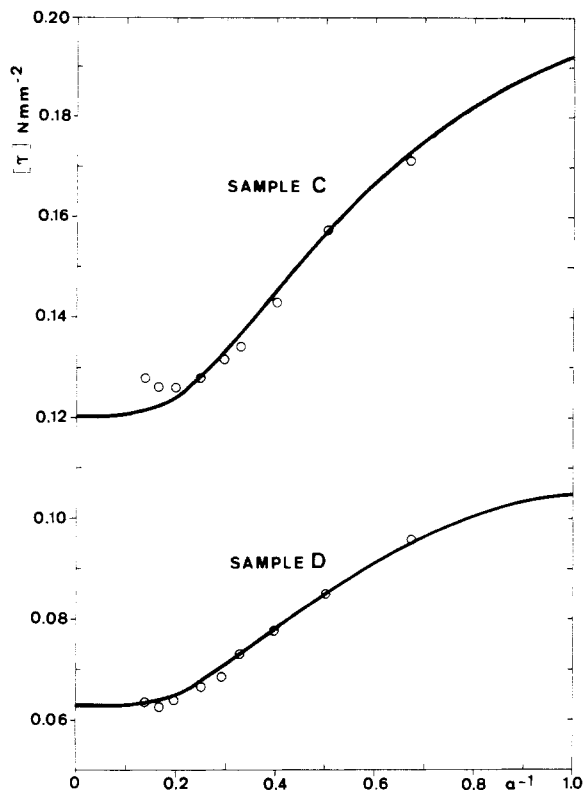


Figure 1. Variation of reduced true stress, $[\tau]$, as a function of reciprocal deformation ratio. Points represent results of experiments for sample C (upper set) and for sample D (lower set). Solid curves are obtained according to the theory. Molecular properties of samples C and D are given in the text, and the parameters used for the theoretical calculations are given in Table I.

Table I
Parameters Used in Theoretical Calculations of Stress and Orientation for the Samples

sample	$\xi kT/V_0$, N mm ⁻²	κ	ζ	$D \times 10^2$	e
A	0.125 ^a	7	0.025	1.30 ^b	1.4
B	0.177 ^a	7	0.025	1.60 ^b	1.4
C	0.121	7	0.025	1.16 ^b	1.4
D	0.063	10	0.025	0.76 ^b	1.6

^a Only the orientation function is calculated in this study for samples A and B; hence the $\xi kT/V_0$ values are not required. They are included in the table for the sake of completeness. ^b At 298 K.

Values of M_c are 2×10^{-4} , 1.5×10^{-4} , 2.2×10^{-4} , and 6.1×10^{-4} for samples A, B, C, and D, respectively. The fluorescence polarization apparatus has been described elsewhere.⁹ It permits simultaneous measurements of stress and orientation during uniaxial stretching at constant crosshead speed, $V = 50$ mm/min, and various temperatures.

Results and Discussion

Characterization of Networks according to Stress-Strain Experiments. Results of stress-deformation measurements on dry samples are shown in Figure 1 in which the reduced stress $[\tau]$ is plotted as a function of α^{-1} , where α is the ratio of the final length along the direction of measurement to the initial length. The reduced true stress $[\tau]$ is defined according to the relation

$$[\tau] = v_2^{-1/3}(\tau_x - \tau_y)/(\alpha^2 - \alpha^{-1}) \quad (1)$$

where $(\tau_x - \tau_y)$ denotes the difference between the true stress along the direction of stretch (x) and the lateral direction (y). v_2 in (1) refers to the volume fraction of polymer in the swollen network. The expression for $(\tau_x - \tau_y)$ in terms of the state of deformation and of the pa-

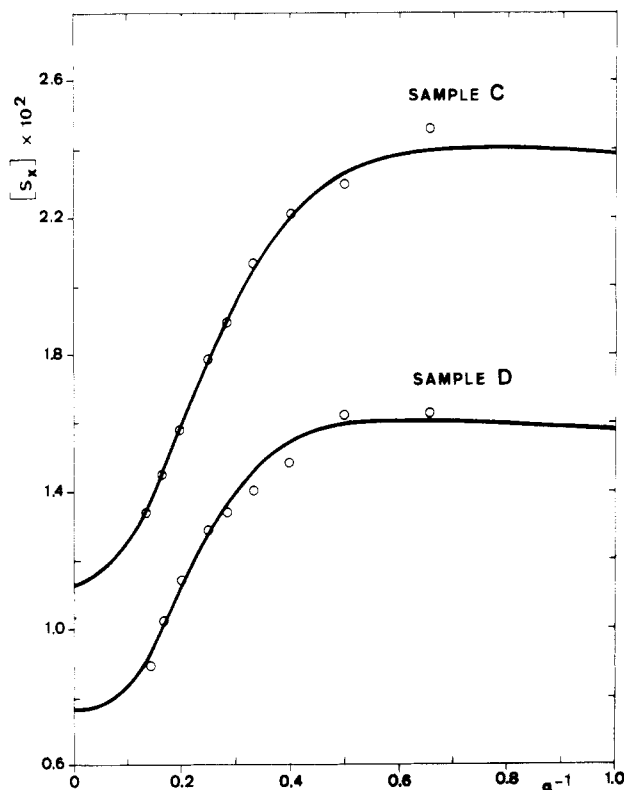


Figure 2. Variation of the reduced orientation function, $[S_x]$, as a function of α^{-1} . Points represent results of experiments for sample C (upper set) and for sample D (lower set). Curves through the points are obtained from theory (see legend of Figure 1).

rameters defining the constitution of the network is given by (I29) (see previous paper in this series¹). Reference to (I29)–(I32) indicates that the constitution of the material is described by three parameters, ξ , κ , and ζ . ξ denotes the number of cyclic circuits of the network and hence is proportional to the modulus of elasticity. κ is a parameter denoting the effect of constraints acting on junctions of the network. It may take a value between 0 and ∞ , the former denoting the phantom and the latter the affine network. The third parameter, ζ , introduces the effects of network inhomogeneities into the theory. Further information on the three parameters, ξ , κ , and ζ are given in ref 1 and the references cited therein.

Data points for two samples, sample C (upper set of points) and sample D (lower set of points), are presented in Figure 1. The curves through the experimental points are obtained by (I29) with $\xi kT/V = 0.12$ N mm⁻², $\kappa = 7$, $\zeta = 0.025$, for sample C and $\xi kT/V = 0.063$ N mm⁻², $\kappa = 10$, $\zeta = 0.025$, for sample D. Values of the three parameters, $\xi kT/V$, κ , and ζ giving the best fit to experimental data are obtained by trial. The value of $\zeta = 0.025$ was required for optimum agreement of the theory with results of orientation measurements (see below). The upturn observed at large α values with sample C could originate from the limited extensibility of network chains. The effect is less apparent in sample D of lower cross-link density.

Dependence of Orientation Function on Strain. The reduced orientation function, $[S_x]$, may be defined as

$$[S_x] = S_x v_2^{2/3} / (1 - 2/\varphi)(\alpha^2 - \alpha^{-1}) \quad (2)$$

Here, S_x denotes the orientation function given by (I27), and φ is the junction functionality. Comparison of (2) with (I27) shows that

$$\lim_{\alpha^{-1} \rightarrow 0} [S_x] = D$$

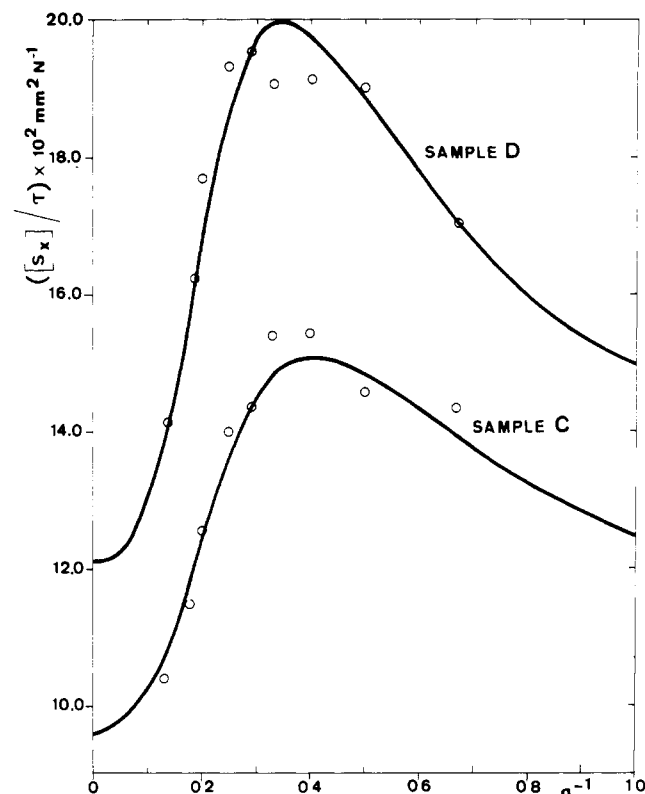


Figure 3. Plot of the ratio of the reduced orientation function to the reduced true stress in terms of α^{-1} . Points are obtained experimentally for sample C (lower set) and sample D (upper set). Curves through the points are obtained from theory (see legend of Figure 1).

Values of $[S_x]$ calculated from experimental measurements are shown in Figure 2 in terms of α^{-1} for samples C and D. The upper set of points refers to results of experimental measurements on sample C and the lower set to those on sample D. Curves through the two sets of points are obtained according to (2) and (I27). The parameters D and e of (I27) are chosen by trial to obtain the best fit to experimental points. A value of $\zeta = 0.025$ was required, as mentioned above, for optimum agreement with data for both samples. For sample C, $D = 1.16 \times 10^{-2}$, $e = 1.4$, and for sample D, $D = 0.76 \times 10^{-2}$, $e = 1.6$, were seen to lead to best fit to experimental results.

According to the two curves obtained by the theory, the reduced orientation function remains approximately constant in the range $1 < \alpha < 2$. Above $\alpha = 2$, the curves steeply converge to the respective phantom values represented by the intercepts at $\alpha^{-1} = 0$.

Ratio of Orientation to Stress. In Figure 3, the ratio of $[S_x]$ to $[\tau]$ is presented for samples C and D. The upper and lower sets of points, referring to samples D and C, respectively, are obtained from experiments. Curves are obtained from the ratios of (2) to (1). The maxima observed in the set of experimental points coincide with the respective maxima in the curves obtained from theory. According to the theory, the limiting value of the intercept of $[S_x]/[\tau]$ at $\alpha^{-1} = 0$ in the absence of local intermolecular correlations should be the same for the two networks since both $[S_x]$ and $[\tau]$ scale with N^{-1} under the stated conditions (where N is the number of segments per chain between cross-links). Experimental values of the intercepts differ by about 20%. Inasmuch as intermolecular correlations do not contribute to stress,³ the observed difference in the ratio $[S_x]/[\tau]$ for the two networks indicates that contribution of intermolecular correlations to segmental orientation is larger in less cross-linked systems.

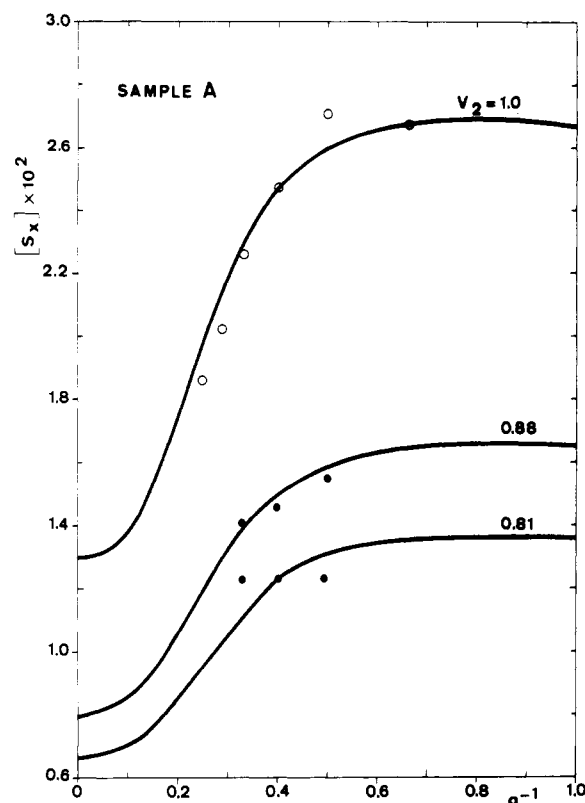


Figure 4. Effect of swelling of segmental orientation. Values of the reduced force are plotted as a function of α^{-1} for sample A. The upper set of circles represents results of measurements on the dry sample. The lower two sets of filled circles represent data for swollen samples. Values of v_2 are shown for each set. Curves through the points are obtained from theory (see legend of Figure 1).

The nonlinearity of the curves and the data points in Figure 3 clearly indicate that orientation is not proportional to stress and that stress cannot be accepted as a measure of segmental orientation in amorphous networks.

Effect of Swelling on Segmental Orientation. Values of the reduced orientation are presented in Figure 4 for sample A. The upper set of points are for the unswollen sample. Inasmuch as the microstructure of sample A is identical with that of sample C, the elastic parameters of the former are adopted for the latter. The solid curve is calculated from (2) and (I27). For best fit to experimental data, values of D and e are chosen, respectively, as 1.3×10^{-2} and 1.4. The value of D chosen is slightly larger than 1.16×10^{-2} , corresponding to that for sample C of the same cross-link density. The lower two sets of filled points in Figure 4 show results of experiments for the same sample A swollen in toluene. The upper set of filled points refers to experiments with $v_2 = 0.88$ and the lower to $v_2 = 0.81$.

Calculations performed by using expressions 2 and I27 show that the absolute value and the α dependence of the reduced orientation $[S_x]$ are insensitive to swelling in the range $0.4 < v_2 < 1$ when e is 1.4. (See Figure 4 of ref 1). Thus, the experimentally observed lowering of $[S_x]$ upon swelling can only be accounted for by considering a decrease in D , reflecting the gradual disappearance of local intermolecular orientational correlations. The theoretical curves drawn through the swollen data according to the theory have been calculated choosing the values of D as 0.8×10^{-2} and 0.66×10^{-2} for $v_2 = 0.88$ and 0.81, respectively. All other parameters in the equations are kept equal to their values for the dry sample. These D values are indicative only. Further experiments with other sol-

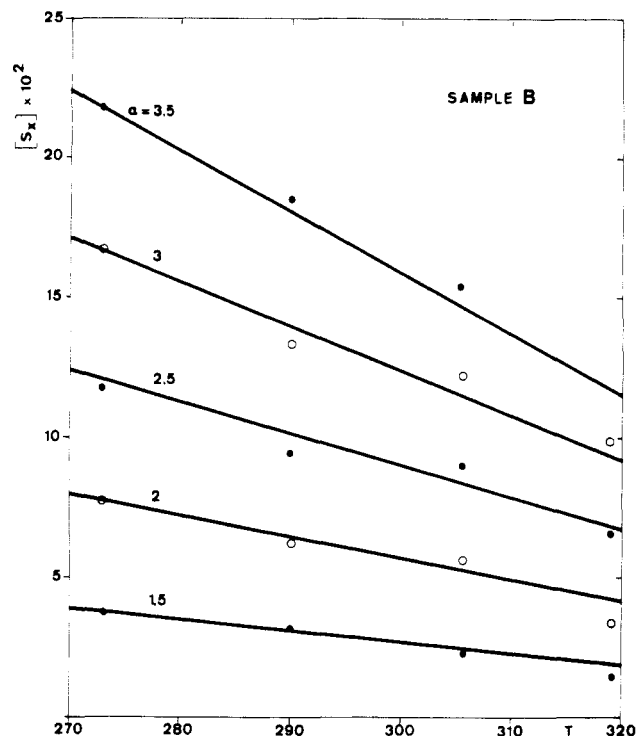


Figure 5. Effect of temperature on orientation, S_x . Filled and empty circles represent experimental data for sample B. Straight lines are obtained from theory. Values of extension ratio, α , for each set of experiments are shown.

vents and using a wide α range are in progress.

Effect of Temperature. Variation of the orientation function with temperature is shown in Figure 5 for sample B. The points show the experimental data at different temperatures in the range $270 \text{ K} < T < 310 \text{ K}$. The straight lines through the points show the best fit calculations according to theory I. The values of κ and ζ were obtained from elasticity measurements as 7 and 0.025, respectively; the value of e was chosen as 1.4, i.e., equal to that obtained for sample A with identical chains. Thus, the only fitting parameter remaining was D . At each temperature of measurement its value was chosen to fit the whole set of data obtained at various values ranging from 1.5 to 3.5. Within the limit of accuracy of the fitting, the effect of temperature on D resulted to be the linear dependence shown in Figure 6. These observed changes in D values may be attributed to the variation of D_{int} with temperature. The absolute values of D_{int} at different temperatures can be extracted from the experimentally determined D values, since D_0 can be calculated at each temperature according to the rotational isomeric state scheme. Calculations along this line are in progress.

It is worthwhile to mention that the present results confirm the qualitative temperature dependence of the intermolecular correlation effect previously reported.^{3,4}

Experimental data reported in this paper and obtained by swelling and/or by varying the temperature of measurements can only be accounted for by changing values of D over a rather wide range (of the order of 2), which reflects the high sensitivity of local intermolecular correlations to these two factors.

Concerning the investigation of solvent effects on these correlations, it is worthwhile to point out that the shape anisotropy of the solvent molecules is of no significance for fluorescence polarization experiments (as well as for infrared dichroism and deuterium NMR spectroscopy). Indeed, their correlations with the network chain segments do not perturb the orientations of the latter. In birefrin-

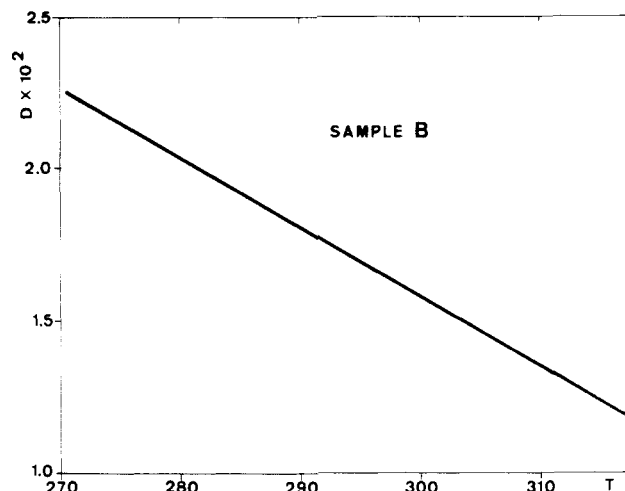


Figure 6. Effect of temperature on the configurational factor, D . The functional relationship of D to temperature is linear as shown, and the method used in its derivation is outlined in the text.

gence measurements, however, alignment of anisotropic solvent molecules along the network chains add to the measured overall birefringence. In this respect, the above-considered spectroscopic techniques appear to be superior to birefringence measurements.

In the case of fluorescence polarization, the fluorescent probe affixed to the chain may be of different chemical structure than that of the main-chain backbone, thus perturbing the state of strain in the surrounding domain, which would otherwise be obtained in its absence. Effects of such perturbations are taken into consideration by adjusting the parameter e . (In IRD and ^2H NMR experiments where molecular structure is not perturbed by the additional label, e should be expected to be smaller but to have the same value for both.) Further perturbations of intermolecular correlations due to the difference of the label from segments of the main chain are of importance also. These latter perturbations should, however, vanish with dilution and temperature. The intramolecular effect of the fluorescent label on D_0 may be calculated precisely by incorporating the necessary statistical parameters arising from the difference of the label into the rotational isomeric state formulation of $\langle r^2 \cos^2 \psi \rangle$ and $\langle r^2 \rangle$.

Experiments performed, but not reported above, on orientation in deformed networks in equilibrium containing fluorescent probes unattached to the network show an orientation of the probes that arises from intermolecular orientational correlations with oriented chain segments.

Acknowledgment. We are indebted to Manufacture Française des Pneumatiques Michelin for samples and helpful discussion. It is also a pleasure to acknowledge the Ph.D. fellowship generously provided J. P. Queslel by Michelin.

References and Notes

- (1) Erman, B.; Monnerie, L. *Macromolecules*, preceding paper in this issue.
- (2) Erman, B.; Flory, P. J. *Macromolecules* 1983, 16, 1607.
- (3) Jarry, J. P.; Monnerie, L. *J. Polym. Sci., Polym. Phys. Ed.* 1980, 18, 1879.
- (4) Queslel, J. P. Thesis, Paris, 1982.
- (5) Erman, B.; Flory, P. J. *Macromolecules* 1983, 16, 1601.
- (6) Monnerie, L. *Faraday Symp. Chem. Soc.* 1983, 18, 57.
- (7) Ward, I. M. "Structure and Properties of Oriented Polymers"; Applied Science: London, 1975.
- (8) Valeur, B.; Monnerie, L. *J. Polym. Sci., Polym. Phys. Ed.* 1976, 14, 11.
- (9) Jarry, J. P.; Sergot, Ph.; Pambrun, C.; Monnerie, L. *J. Phys. E* 1978, 11, 702.